

Coupled Tilt and Translational Ground Motion Response Spectra

Erol Kalkan¹ and Vladimir Graizer²

Abstract: Dynamic response of structures subjected to earthquake-induced base excitations are often simplified by ignoring the tilt components of ground motion. However, close to the earthquake source, tilting of the ground surface may become significant. Based on strong-motion records at the Pacoima Dam—upper left abutment obtained during the 1994 Northridge Earthquake, residual tilt reached 3.1° in the N45°E direction while the dynamic tilt remained higher. This study investigates the consequences of neglecting the effects of the tilt component in ground motions on elastic and inelastic spectral ordinates. A complete equation of motion for a single-degree-of-freedom (SDOF) oscillator is developed which includes the effects of tilt (as the secondary $P-\Delta$ effect) in addition to inertial force effects due to angular and translation accelerations. The expected values of the largest response peaks are computed for the translational and tilting excitations to investigate the relative contribution of each forcing function. The coupled tilt and translational ground motion response spectrum (CTT spectrum) is generated considering elastic and inelastic response of SDOF oscillator. The CTT spectrum reflects kinematic characteristics of the ground motion that are not identifiable by the translational ground motion response spectrum alone and therefore emerges as a distinct intensity measure of translational ground motion when it is coupled with dynamic tilting of the ground surface on the order of few degrees.

DOI: 10.1061/(ASCE)0733-9445(2007)133:5(609)

CE Database subject headings: Ground motion; Earthquakes; Rotation; Response spectra; Coupling.

Introduction

Propagation of elastic waves generated by an earthquake source produces horizontal and vertical movements of the ground surface, complete characterization of which can only be achieved by measuring three rotational (θ_x , θ_y , and θ_z) and three translational degrees of freedom (x , y , and z) in the Cartesian coordinate system. Dynamic response calculations of structural systems however, are often simplified by ignoring rotational components of ground motion. This has been a widely accepted practice in the engineering community due to a lack of recorded rotational components of ground shaking and a common assumption in the seismological community that rotational components are small enough to neglect. As opposing, along the edges of fault planes and near abrupt changes of fault slip, tensile fractures can contribute to the radiation of rotational waves (Takeo and Ito 1997). Consequently, tilting of the ground surface may become significant close to the earthquake source. For instance, the great Alaska Earthquake (1964) tilted an area of at least 120,000 km² and resulted in relative land subsidence as much as 2.5 m. During the M7.2 earthquake in the Gulf of Corinth (Greece), vertical move-

ment was restricted mainly to a relatively narrow crustal zone and has resulted in northward and southward tilting (Tselentis and Makropoulos 1986). A more localized, yet dramatic case was observed during the Mw 6.7 1994 Northridge Earthquake at the Pacoima Dam—upper left abutment where the residual tilt reached 3.1° in the N45°E direction (Graizer 2006b).

Current horizontal pendulum seismometers cannot directly distinguish between tilt components and translational accelerations, and their record amplitudes are proportional to the combination of translational motion and tilt. To be more specific, tilting of the ground beneath the instrument may shift the baseline of the horizontal pendulum, and by virtue of rotational inertia the instrument may also respond to a rotational motion. In such case, a recording interpreted as “horizontal acceleration” is not a pure horizontal motion and may be significantly contaminated by a rotational component through long-period wave penetration effects. For this reason, accelerograms contaminated by a tilt component may need baseline correction and low-cut filtering. Strong-motion records contaminated by tilt make calculation of a displacement, including residual almost impossible (Graizer 2005) unless there is supplementary data from GPS measurements before and after earthquakes to be used in calibrating the signal processing filters. In case of lacking such data, it is more appropriate to process records with a procedure similar to that developed by Trifunac (1971).

Studies by Bouchon and Aki (1982), Lee and Trifunac (1985) and Castellani and Boffi (1986) indicated that rotational ground motion could be important in the near-field and for surface waves. Stratta and Griswold (1976), Ghafory-Ashtiany and Singh (1986), and Gupta and Trifunac (1991) emphasized the possible effects of a rotational component of motion on building response. Several investigators have also attempted to indirectly estimate the rotational components. Based on the elastic-wave theory, Lee and

¹California Geological Survey, Sacramento, CA 95814-3500 (correspondence author). E-mail: ekalkan@consvr.ca.gov

²California Geological Survey, Sacramento, CA 95814-3500. E-mail: vgraizer@consvr.ca.gov

Note. Associate Editor: Vinay Kumar Gupta. Discussion open until October 1, 2007. Separate discussions must be submitted for individual papers. To extend the closing date by one month, a written request must be filed with the ASCE Managing Editor. The manuscript for this paper was submitted for review and possible publication on March 20, 2006; approved on September 29, 2006. This paper is part of the *Journal of Structural Engineering*, Vol. 133, No. 5, May 1, 2007. ©ASCE, ISSN 0733-9445/2007/5-609-619/\$25.00.

Trifunac (1987) were able to generate synthetic accelerograms for rotational degree-of-freedom associated with plane P , SV and Rayleigh waves. Following the same idea, an improved approach to estimate the rotational components of motion from recorded orthogonal translational components has been proposed by Li et al. (2004). However, these methods are applicable for accelerograms recorded in the far-field due to complex wave propagation mechanisms in the vicinity of active faulting. Rotational components have also been estimated using measured linear accelerograms from dense arrays by Niazi (1986), and Oliveria and Bolt (1989). Although some efforts have been recently devoted to directly measure six components of ground motion (e.g., Nigbor 1994), there is still lack of direct broadband recorded data close to the earthquake source. While the rotation component of the motion is related to spatial variation of ground motion (e.g., Harichandran 1991), use of closely spaced accelerometer arrays to measure rotations is now a main effort in the scientific community (see e.g., Zerva and Beck 2003; Hao et al. 1989).

In this paper, a procedure is presented to recover the long-period component of tilt motion using the accelerograms recorded by a conventional triaxial seismometer. The procedure was initially proposed by Graizer (1989) and is based on a difference in the tilt sensitivities of the horizontal and vertical pendulums. The procedure was tested in a number of laboratory experiments with different strong-motion accelerographs put on shake tables (Graizer 2006b). Its accuracy in estimating the residual ground tilting is verified in this study against the field measurement conducted at the Pacoima Dam—upper left abutment recording station after the Northridge Earthquake.

To examine the possible effects of ground tilting on the response of a single-degree-of-freedom (SDOF) oscillator, the complete equation of motion is developed including combined effects of angular and translational accelerations. Forcing functions of the dynamic equilibrium equation include the secondary P – Δ component caused by tilt effect and inertial force components due to angular and translational accelerations. The expected values of the largest response peaks are computed for the translational and for the tilting excitations to investigate the comparative contribution of each forcing function to the overall response of a SDOF oscillator. To represent the peak response values in a generic spectral format, the coupled tilt and translational response spectrum (CTT spectrum) is produced, considering elastic and inelastic systems having constant-ductility demands. The proposed CTT spectrum reflects the kinematic characteristics of the ground motion that are not identifiable by the translational response spectrum alone and therefore emerges as a distinct intensity measure of translational ground motion when it is coupled with dynamic tilting of the ground surface on the order of few degrees. Finally, the conceptual details of coupled tilt and translational motions with rocking response associated with soil-structure interaction (SSI) effects are discussed.

Triaxial Seismometer Response to Ground Shaking

As shown in Graizer (1989, 2005), the differential equation of small oscillations of horizontal pendulum motion can be written as

$$\ddot{y}_1 + 2\omega_1 D_1 \dot{y}_1 + \omega_1^2 y_1 = -\ddot{x}_1 + g\psi_2 - \ddot{\psi}_3 l_1 + \ddot{x}_2 \theta_1 \quad (1)$$

where y_i =recorded response of the instrument; θ_i =angle of pendulum rotation; l_i =length of pendulum arm; ω_i and D_i =the natu-

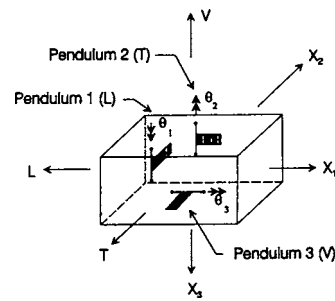


Fig. 1. Oscillation directions of transducers within an accelerograph in three-dimensional space (letter in parentheses indicates the direction of movement)

ral frequency and fraction of critical damping of the i th transducer, respectively; g =gravitational acceleration; \ddot{x}_i =ground acceleration in the i th direction; and ψ_i =rotation of the ground surface about x_i axis. Note that Eq. (1) is derived based on Cartesian coordinate system in three-dimensional space as shown in Fig. 1.

Sensitivity of the vertical pendulum to tilts is different. For small tilts, it is proportional to $[1 - \cos(\psi)]$ and $\cos(\psi) \approx 1 - \psi^2/2$. Then, the equation of the vertical pendulum can be written as follows:

$$\ddot{y}_3 + 2\omega_3 D_3 \dot{y}_3 + \omega_3^2 y_3 = -\ddot{x}_3 + g\psi_1^2/2 - \ddot{\psi}_1 l_3 + \ddot{x}_2 \theta_3 \quad (2)$$

Neglecting $g\psi_1^2/2$ yields

$$\ddot{y}_3 + 2\omega_3 D_3 \dot{y}_3 + \omega_3^2 y_3 = -\ddot{x}_3 - \ddot{\psi}_1 l_3 - \ddot{x}_2 \theta_3 \quad (3)$$

Thus, a horizontal pendulum [Eq. (1)] is sensitive to the acceleration of linear motion, tilt, angular acceleration, and cross axis excitations. The difference in tilt sensitivity of vertical and horizontal pendulums is well known by the instrument designers, but is usually ignored in data processing and analysis. For a correct interpretation of strong-motion recordings, it is important to study the sensitivity of a pendulum to the second, third and fourth terms on the right-hand side of Eqs. (1) and (3). Possible impacts of different terms in the right-hand side of Eqs. (1) and (3) were studied by Wong and Trifunac (1977), Graizer (1989, 2006a), Todorovska (1998), and Trifunac and Todorovska (2001). Based on numerical simulations performed for a number of typical strong-motion instruments, Graizer (1989, 2005) concluded that tilts could influence significantly the output of the horizontal pendulums. The effect of angular acceleration is significant for instruments with a long pendulum arm l_i , as in the case of some classical seismometers, but is small for typical accelerometers with a short pendulum arm. The effect of cross-axis sensitivity may reach a few percent for accelerations higher than 2 g , and for accelerometers with a natural frequency of 25 Hz. Cross-axis sensitivity is almost negligible for modern accelerometers that have a natural frequency of about 100 Hz and a short pendulum arm. The terms caused by tilting are always present for the horizontal pendulum, and cannot be neglected.

For small oscillations of a pendulum with a short pendulum arm, the vertical accelerometer is almost insensitive to tilts and neglecting the cross-axis sensitivity terms, the differential equations of the horizontal and vertical pendulums simplify to

$$\ddot{y}_1 + 2\omega_1 D_1 \dot{y}_1 + \omega_1^2 y_1 = -\ddot{x}_1 + g\psi_2 \quad (4)$$

$$\ddot{y}_3 + 2\omega_3 D_3 \dot{y}_3 + \omega_3^2 y_3 = -\ddot{x}_3 \quad (5)$$

Thus, in a typical strong-motion triaxial instrument, the two horizontal sensors are responding to the combination of inputs corresponding to horizontal accelerations and tilts, whereas the vertical sensor is mainly responding to the vertical acceleration. The horizontal sensor [Eq. (4)] is sensitive to the second derivative of displacement and to tilt. This means that a double integration of Eq. (4) will produce the sum of displacement and double integrated tilt. Assuming that tilt is proportional to velocity (Bouchon and Aki 1982; Trifunac and Todorovska 2001), double integration will give results proportional to the integral of displacement, and the result can look like long-period noise. Recently, Zahradnik and Plesinger (2005) have suggested that local tilts triggered by high-frequency ground vibration may be the source of long-period pulses in broadband records of earthquakes recorded in the near field.

Recovering Tilt Motion

The method of tilt recovering using accelerograms is based on the difference in the tilt sensitivity of the horizontal and vertical pendulums [Eqs. (4) and (5)]. The method was first suggested by Graizer (1989) and tested in a number of laboratory experiments with different strong-motion accelerographs (Graizer 2006b). A first set of experiments was performed with a specially designed shake table at the Institute of the Physics of the Earth in Moscow in 1987. The second group of tests was conducted with Willie Lee at the U.S Geological Survey Menlo Park in 1993.

Methodology

In the near-field of the source, a displacement signal may contain oscillative and residual parts. The Fourier spectrum of the near-field displacement will increase with the decrease of the frequency, and the velocity spectrum will be flat at low frequencies. Consequently, the acceleration spectrum will increase with the frequency from zero till the maximum at a few hertz. It is also known that the Fourier spectra of vertical and horizontal components of acceleration demonstrate differences in the high frequency range (above a few hertz). The spectra of the ideal vertical and horizontal components of acceleration in the frequency domain from zero-frequency to a few hertz should be similar in shape, with the horizontal spectrum being usually about twice as high as the vertical. As was shown by Bouchon and Aki (1982), the vertical component's velocity in the near-field of a strike-slip fault is similar in shape to the tilt component. Evidently in this case, the tilt's Fourier spectrum will be similar to the spectrum of the vertical component of ground velocity. Since the response of the vertical pendulum is proportional to translational motion only, the acceleration spectrum should increase from zero frequency to a maximum at a few hertz. In contrast to the vertical, the horizontal pendulum's spectrum is a combination of translation and tilt. If tilt is negligible, it should behave the same way as the vertical spectrum at low frequencies. If tilt is present (and is large enough), the low frequency part of the Fourier spectra will be flat at low frequencies (same as the tilt spectrum's behavior). The low frequency part of the horizontal pendulum spectrum in this case is controlled by tilt. Therefore, based on Eqs. (4) and (5), one can expect to see the similar low frequency content in the true vertical and horizontal motions recorded by triaxial accelerograms. If the

recorded level of long-period motion is significantly higher in the horizontal components, this could possibly be due to tilts.

The procedure of tilt recovering includes the following steps:

1. Compute the smoothed Fourier spectra for uncorrected vertical and horizontal components.
2. Calculate the ratio of the horizontal-to-vertical Fourier spectra.
3. Choose the characteristic frequency. At frequencies lower than the characteristic one, the horizontal component's spectrum is several times higher than that of the vertical.
4. Filter the horizontal component of acceleration using the characteristic frequency computed at Step 3. The applied filter of low frequencies (FLF=high-cut filter) filters out all frequencies higher than the characteristic frequency. An assumption is made that the filtered signal is proportional to tilt.

In real applications, it is recommended to run a few corner frequencies, and select a solution that satisfies to the best of our knowledge about the shape of the tilt function. Depending upon the task, it is possible to apply different types of filters such as physically realized (causal) FLF or an acausal FLF (the same causal filter applied twice: in forward and backward directions to avoid phase shift). Although the applicability of the methodology described above has been tested numerically and also experimentally in a shake table experiments for a number of strong motion records reported in Graizer (2006b), its application is best exemplified on a ground motion recorded at the Pacoima Dam station in the following.

Example Case: Pacoima Dam—Upper Left Abutment

This station recorded strong motions from two major earthquakes: San Fernando in 1971 and Northridge in 1994. According to Trifunac and Hudson (1971), the instrument experienced tilt on the order of 0.5° during the former event. During the latter event, Shakal et al. (1994) reported that it also experienced tilt. The residual tilting angle of the strong-motion instrument was measured as 3.5° in the N40°E direction (down slope direction of the ridge) by the California Strong Motion Instrumentation Program (CSMIP) few days after the earthquake.

To recover the tilt component, the method described previously is applied to recorded raw data. The 20 s long intervals of the recordings were used because it is the length of the first digitization panel (see Fig. 2). In this case there is no need to deal with results of panel matching that can possibly produce fictitious tilt. Fig. 3 compares the ratios of horizontal-to-vertical Fourier amplitude spectra for the components oriented along 210 and 120°. The uncorrected record of the 210° component demonstrates a significantly higher predominance of low-frequency contents. It also has a visible shift of the zero acceleration level. Filtering this component results in an estimated tilt response of 3.4 (maximum) and 3.1° of residual tilt (Fig. 4).

The 120° component demonstrates less significant predominance at lower frequencies than the 210° (at frequencies lower than 0.2 Hz). Filtering of the 120° component produces a much lower value of residual tilt of about −0.80° (Fig. 4). This value should probably be considered much less reliable than that of the 210° component since it is closer to the noise level in these records.

If we assume that both estimated tilt values (3.1° tilt along the 210° component and −0.80° tilt along the 120° component) are reliable, it is possible to obtain the vector orientation and value of tilt. Since the positive tilting corresponds to uplifting, one can

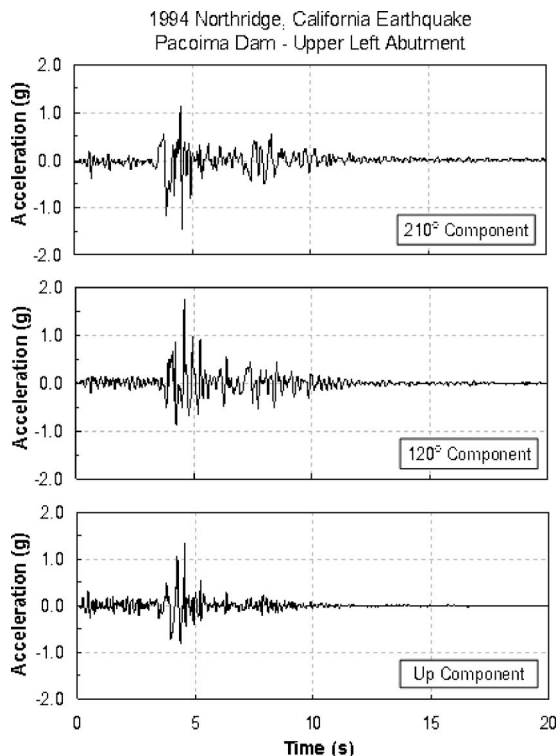


Fig. 2. Recorded strong ground motion (uncorrected) at Pacoima Dam—upper left abutment

conclude that uplifting occurred in the 225° direction. Consequently, actual tilting occurred in the $N45^\circ E$ azimuth with amplitude of about 3.1° .

The tilt motion function obtained from the acceleration record demonstrates tilt rising from zero to the level of about 3.1° in a time period of 3.5 to 8 seconds from the beginning of recording. Main tilt increase (step-type function) correlates well with the highest level of recorded acceleration. Main tilt occurred with the arrival of the strong phase of the *S* wave. Estimated velocity of tilting results in a maximum amplitude of about $15^\circ/s$ or 0.3 rad/s (see Fig. 5). Residual tilt of about 3.1° produces the same result in accelerometer response as an acceleration of about 0.05 g . This value of residual tilt of about 3.1° is in good agreement with the residual tilt of 3.5° measured independently by CSMIP.

Fig. 6 demonstrates the comparison of spectra of the vertical component of acceleration with that of the estimated velocity of tilting. The high-frequencies parts ($>10 \text{ Hz}$) of the spectra are very similar, but the low-frequency parts demonstrate differences due to the residual tilt.

Single-Degree-of-Freedom Oscillators

Behavior of a SDOF oscillator used in structural engineering differs slightly from that of a pendulum utilized in strong motion recording instruments due to orientation and damping. Compared to vertically oriented SDOF oscillators, pendulums are located horizontally in the strong motion instrument, and move in either the horizontal or vertical plane (Fig. 1). This configuration ideally eliminates the destabilizing effect of gravity, provided that there is no tilting in the three-degree-of-freedom plane. In addition, pendulums in seismological instruments have very high damping ra-

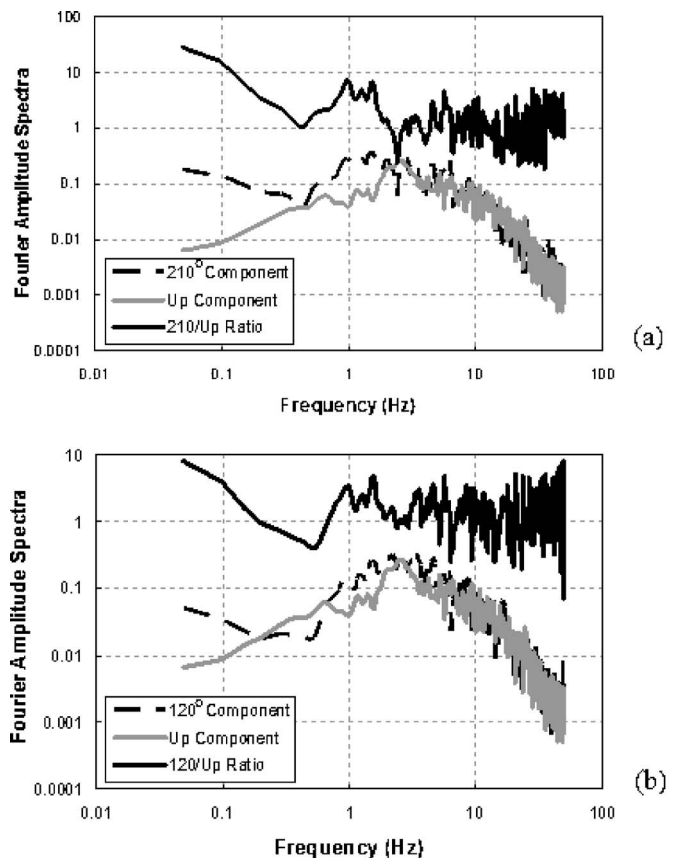


Fig. 3. Fourier amplitude spectra for the components oriented along (a) 210° ; (b) 120°

tios close to 70% of the critical damping, as opposed to a lower damping ratio (generally 5% percent) of SDOF oscillators used as representatives of multi-degree-of-freedom systems. In the following, the response of a SDOF oscillator to pure translational ground motion is first revisited and the dynamic response of a SDOF oscillator to coupled tilt and translational ground motions is derived.

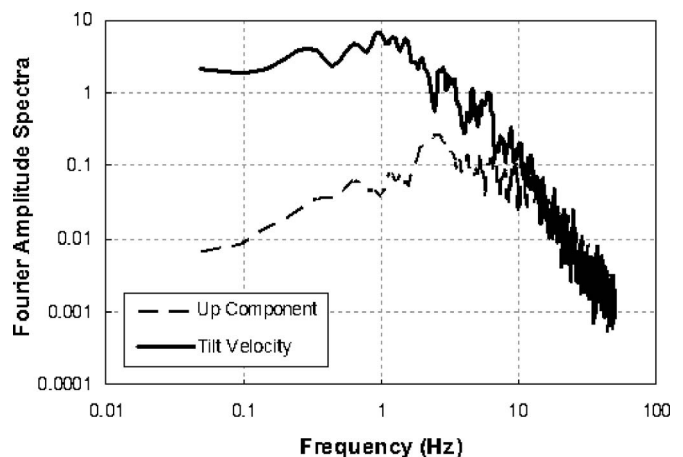


Fig. 4. Estimated tilt

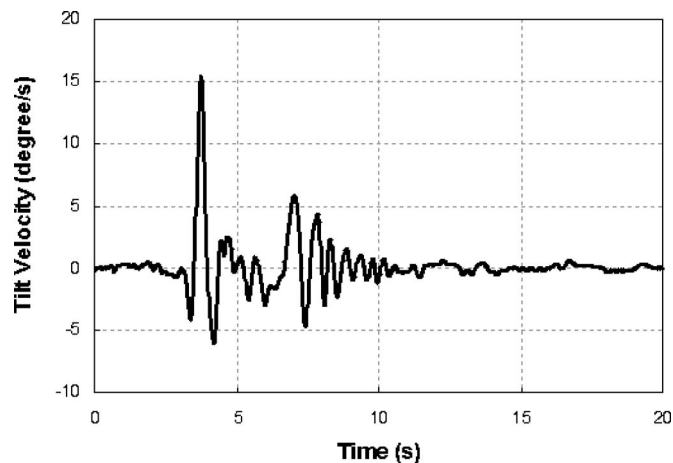


Fig. 5. Estimated velocity of tilt for 210° component

Response to Pure Translational Ground Motion

Dynamic equilibrium of the mass m of the SDOF oscillator with stiffness, k and damping, c shown in Fig. 7(a) yields

$$m\ddot{u} + c\dot{u} + ku = -m\ddot{u}_g \quad (6)$$

where u =relative displacement of the oscillator with respect to ground and \ddot{u}_g =ground-induced translational acceleration. For the sake of simplicity, a SDOF oscillator is represented by a rigid bar and system flexibility is lumped in a rotational spring at the base. The initial stiffness of the system is denoted as k_0 and the stable bilinear material model with post yield stiffness ratio of κ is assumed. The resistance force, V is a function of relative displacement, u . The force–deformation plot in Fig. 7(a) indicates the response of a SDOF oscillator to translational motion whereby the destabilizing effect of axial load (i.e., P – Δ effect) in the deformed position is ignored. As shown, u can be computed as ϕ/l for small angles ($\sin \phi \cong \phi$).

The P – Δ effects on the response is considered in Fig. 7(b) in which the secondary moment, created by axial load times relative displacement u , is represented by an equivalent force-couple acting on the mass of the system as $mg\phi$. As ϕ is a function of the response parameter u , it is more convenient for numerical computations to cast this additional forcing function in a geometric

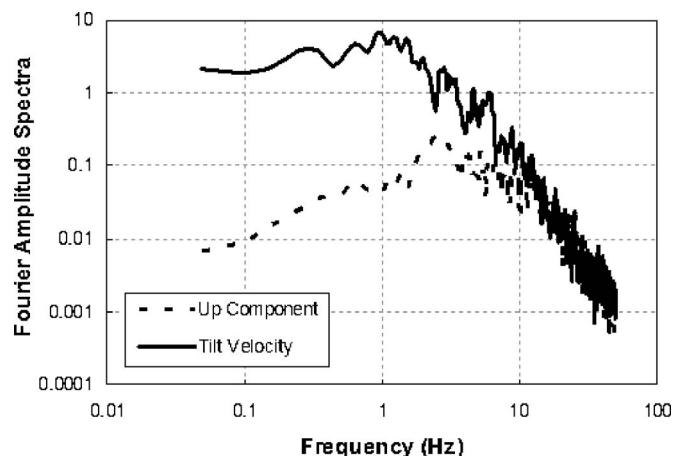


Fig. 6. Comparison of Fourier amplitude spectrum of the vertical component of acceleration with that of the estimated velocity of tilt

stiffness term, k_g ($k_g = mg/l$) on the left-hand-side of Eq. (6). The ratio of the geometric stiffness term to initial stiffness yields the well-known stability coefficient, θ

$$\theta = k_g/k_0 \quad (7)$$

The stiffness apparent in the second-order analysis is called as an effective stiffness. In the preyield condition, it is equal to $k=k_0(1-\theta)$, whereas in the postyield condition it can be expressed as $k=k_0(\kappa-\theta)$. Thus, the effective period of the structure, T , accounting for P – Δ effects, reads

$$T = T_0/\sqrt{1-\theta} \quad (8)$$

where T_0 is based on the initial stiffness of the first order analysis. In contrast to the first order, second order analysis of structures considers equilibrium in the deformed position, because the instability may arise when the θ approaches θ_{equil} , which is the solution of $k(u)\theta_{\text{equil}} = mgh(\sin \theta_{\text{equil}})$. The dynamic equilibrium equation nesting P – Δ effects in the geometric stiffness term can be expressed as

$$m\ddot{u} + c\dot{u} + (k_0 - k_g)u = -m\ddot{u}_g \quad (9)$$

For nonlinear response, Eq. (9) can be solved incrementally in the time domain by replacing k_0 by instantaneous tangent stiffness that varies according to hysteretic behavior of the system. Unlike tangent stiffness, the geometric stiffness term remains unchanged in the inelastic range. It is also instructive to note that initial period and effective stiffness vary by including the P – Δ effects. On the other hand, yield displacement (u_y) remains similar, as u_y is directly related to moment-curvature behavior at the section level, whereas P – Δ becomes effective in the global system level.

Response to Coupled Tilt and Translational Ground Motions

To fully understand the response of a SDOF oscillator to tilt motion, it is convenient to examine the P – Δ effects separately. First let us think of a SDOF oscillator with a concentrated mass and height (l) as illustrated in Fig. 8(a). When it is subjected to base rotation only, the oscillator mass is influenced by the inertial force (F_α) due to the angular acceleration ($\ddot{\alpha}$) expressed as

$$F_\alpha = m\ddot{\alpha}l \quad (10)$$

It is possible to represent the rotating-base oscillator in Fig. 8(a) with an equivalent fixed-base oscillator as illustrated in Fig 8(b). This representation has some computational advantages especially for inelastic systems. It provides directly the relative drift associated with the exact deformation. The response of an equivalent fixed-base oscillator therefore does not include the rigid body rotation (α), yet it includes its forcing effects. It means that relative rotations (ϕ) of rotating-base and fixed-base oscillators become identical while the total rotation of a fixed-base oscillator can be obtained explicitly by summing α (i.e., base tilting) and ϕ .

When the rotating-base oscillator is subjected to coupled tilt and translational components of ground motion, then resultant reacting forces on the corresponding equivalent fixed-base oscillator can be represented by superposing two inertia forces originated by translational and angular accelerations (i.e., $m\ddot{u}_g + m\ddot{\alpha}l$).

As evident in Fig. 8(a), additional rigid body rotation due to base tilting amplifies the P – Δ effects by increasing the moment arm. In this case, it is convenient to decompose the total P – Δ contribution into two components. The first component originates

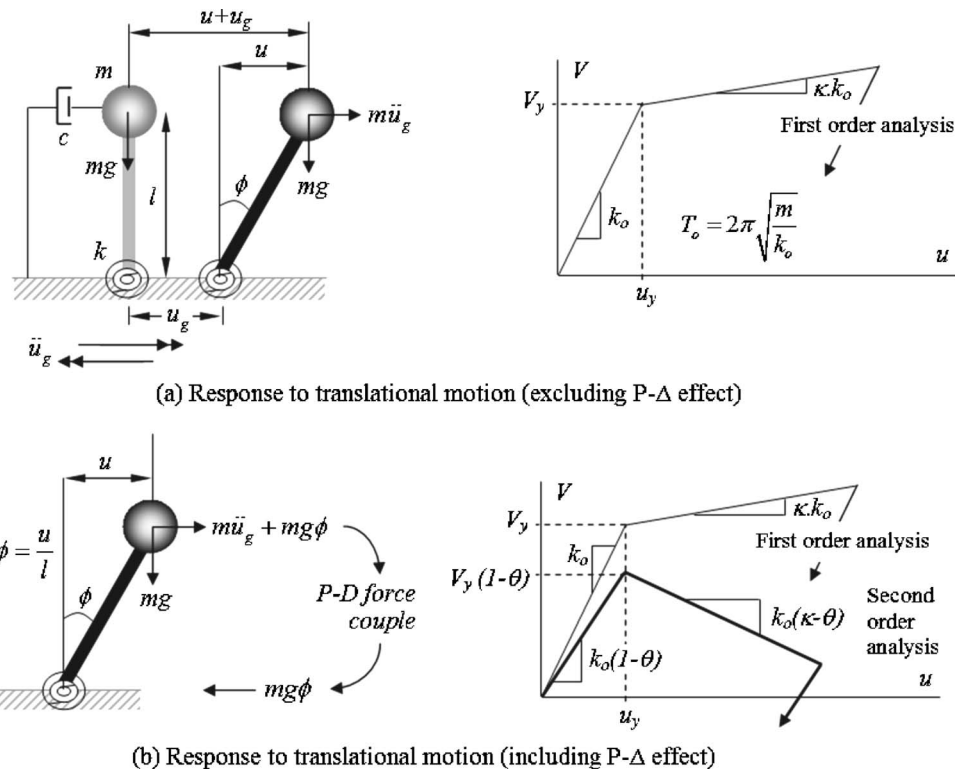


Fig. 7. Fixed-base SDOF oscillator subjected to translational ground motion

due to base tilting (α) which can be represented as an additional forcing function since it is independent of oscillator response, while the second $P-\Delta$ component is a direct consequence of relative oscillator response (ϕ), therefore it can be treated within the geometric stiffness term (k_G). Again, the total rotation of a fixed-base oscillator can be obtained by adding the base rotation (α) to the system relative rotation (ϕ). Fig. 8(b) illustrates complete forcing functions acting on the mass of the equivalent fixed-base oscillator when it is subjected to coupled tilt and translational motions. The corresponding dynamic equilibrium equation of this physical system can be written as

$$m\ddot{u} + c\dot{u} + ku = -(m\ddot{u}_g + mg\phi + mg\alpha + m\ddot{\alpha}l) \quad (11)$$

Eq. (11) can also be derived using Lagrange formulation through equilibrium of potential and kinetic energies. By representing the $P-\Delta$ component due to ϕ in k_G , the Eq. (11) can be alternatively expressed in the following form

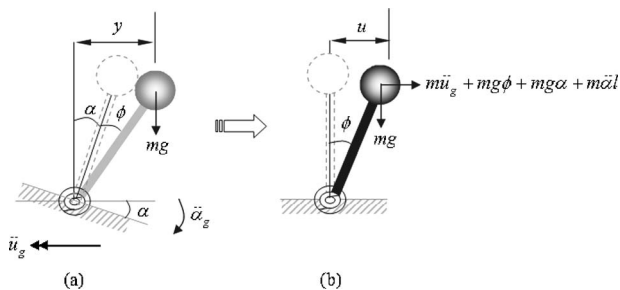


Fig. 8. (a) SDOF oscillator subjected to coupled tilt and translational ground motion; (b) equivalent fixed-base system

$$m\ddot{u} + c\dot{u} + (k_0 - k_G)u = -(m\ddot{u}_g + mg\alpha + m\ddot{\alpha}l) \quad (12)$$

Depending on the sign convention for angular and translational acceleration, the sign of forcing functions in Eqs. (11) and (12) may change (see Fig. 8 for the compatible sign convention used in derivation of these equations). It should be also noted that Eqs. (11) and (12) neglect the effects of vertical ground acceleration, which, for large α may lead to dynamic instability (e.g., see Lee 1979).

Fig. 8(a) clearly indicates that considering the tilt component not only brings an additional lateral force due to angular acceleration, but also increases the $P-\Delta$ effects. Such a combination may induce asymmetric behavior and consequently causes a reduction in the resistance of a structure to the amplified applied lateral forces. This phenomenon is numerically exemplified for a SDOF oscillator subjected to the strong motion record of Pacoima Dam—upper left Abutment in Fig. 9. The velocity time-series of the translational component of the record is plotted in Fig. 9(a), whereas its tilt component is shown in Fig. 9(b). It is also instructive to note that the arrival of the initial major velocity pulse as the time integration of distinguishable acceleration pulse in the acceleration time-series (see Fig. 2 for 210° component) is well synchronized with the step rise in the tilt motion. Corresponding impacts of dynamic tilt on the displacement demand of the SDOF oscillator is studied comparatively in Figs. 9(c and d). To simplify the presentation, the SDOF oscillator is modeled with a stable bilinear hysteretic behavior with a kinematic strain hardening ratio (κ) of 0.01 and a stability coefficient (θ) of 0.17. Its initial period (T_0) is 1.0 s whereas its effective period (T_{eff}) is 1.1 s due to the $P-\Delta$ effect. Damping of the system is taken as 5% of critical damping. The displacement values ($u = \phi l$) plotted in Fig. 9(c) are relative values computed based on relative rotation of the oscillator's mass with respect to its base; therefore they include

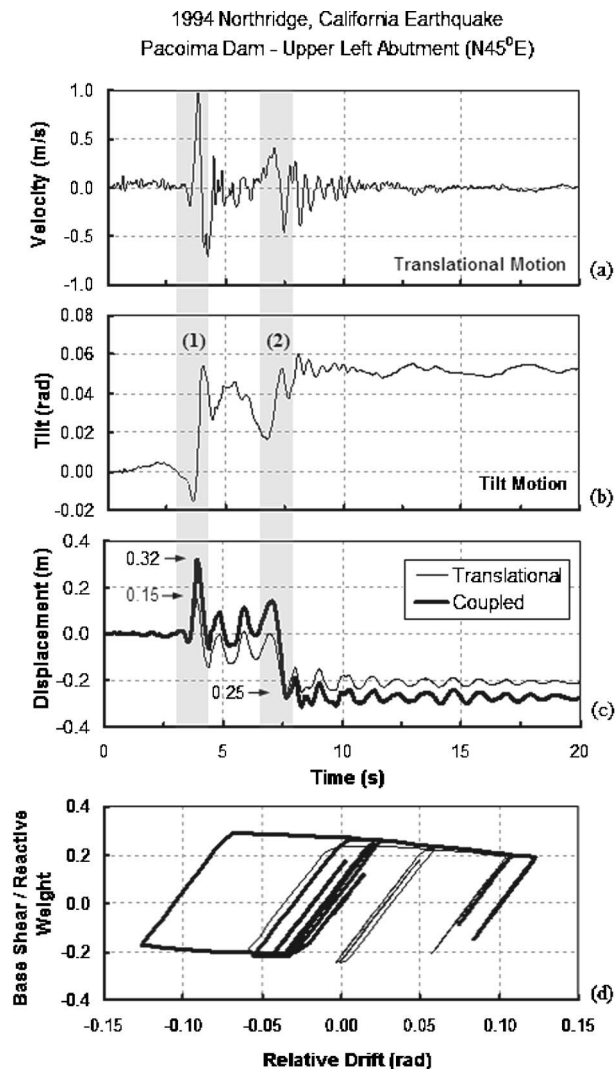


Fig. 9. Comparison of SDOF oscillator time-response to pure translational and coupled translational and tilt motions (shaded area denotes the first and second major velocity pulse arrivals)

neither the rigid body translation (u_g), nor the rigid body rotation (α). As shown, the tilt component has significant influence to escalate the peak displacement demand. This peak demand takes place in the same direction of tilting of ground within a single cycle synchronized with initial distinct velocity pulse arrival (follow the shaded area-1 in Fig. 9). Following the step-rise in the tilt component of motion, the SDOF oscillator responds to the rest of the motion in a tilted position. With the arrival of a second velocity pulse (shaded area-2 in Fig. 9), oscillator moves to opposite direction in a single plastic cycle and continues to oscillate in this deformed position without experiencing any more plastic deformation. The residual displacement of the system is also increased due to tilt compared to the response of the oscillator to pure translational motion. In both cases, the overall response of the oscillator is dominated by two plastic cycles associated with two distinct velocity pulses contained in the record.

Fig. 9(d) illustrates the load-deformation time-history for two cases with and without tilt motion. In Fig. 9(d), the y-axis indicates the normalized base shear (or acting force on mass) with reactive weight (W) and relative drift stands for relative displacement (u) normalized by height (l) (i.e., relative rotation of the

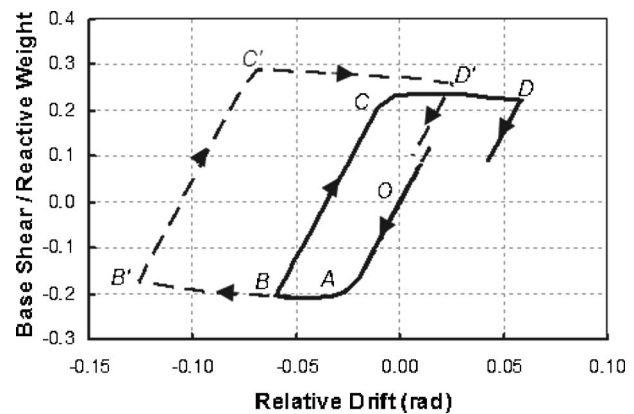


Fig. 10. A close-up view to first cyclic response (duration window is 0 to 4.5 s; dashed line=response to coupled tilt and translational motion, continuous line=response to pure translational motion only)

system in radian, ϕ). $P-\Delta$ effects associated with tilt can exert large influence on the dynamic response, particularly for systems that deform beyond the yield point and create negative tangent stiffness in the postyield deformation range by offsetting the effects of strain hardening. Without having instability, maximum ductility of SDOF oscillators in case of coupled tilt and translational motion extends to 6.3, whereas applying pure translational motion limits the ductility demand to 3.2. For a structure exhibiting satisfactory performance, its seismic design should provide adequate stiffness and strength so that its ultimate ductility level should not exceed its maximum ductility under design level seismic excitation. Using the above as a performance evaluation criterion, a structure exhibiting satisfactory seismic performance under translational motion may go into collapse when a translational motion is coupled with ground tilting of a few degrees.

More insight into the dynamic behavior of a SDOF oscillator under the influence of tilt motion is provided in Fig. 10. This figure focuses on the first cyclic response associated with the peak observed demands [see also Fig. 9(c)]. This is a typical behavior imposed by pulse-type near-fault records, whereby most of the seismic energy is imparted to the structural system through a single “effective cycle” (Kalkan and Kunnath 2006, 2007). As seen in Fig. 10, the first yielding takes place at Point A. For the system subjected to pure translational motion without tilt, stored strain energy in the system is not sufficient to push it beyond Point B on the way to Point B', therefore kinetic energy of the system ceases at Point B (i.e., $\dot{u}=0$) and the system returns back (unloading) with a change in sign of \dot{u} . If the tilt component of motion is applied together with the translational component, additional $P-\Delta$ effect and inertial force due to angular acceleration cause the system to advance inelastically to the right (negative u direction), pass Point B and reach to Point B'. The bias toward increasing displacements in one direction becomes greater as the current ductility of the system increases and as the postyield tangent stiffness becomes increasingly negative. This has important practical implications, such as dynamic instability (or collapse) could be triggered if the energy of coupled tilt and translational motion was large enough to carry the system inelastically beyond Point B' to produce more asymmetric deformation accumulation.

The tendency of asymmetric deformation due to the tilt component is studied next in Fig. 11 where a SDOF oscillator with a similar effective period, yet having 40% less yield strength (to generate more plastic deformation), is subjected to the Pacoima Dam record with and without a tilt component. It is evident that

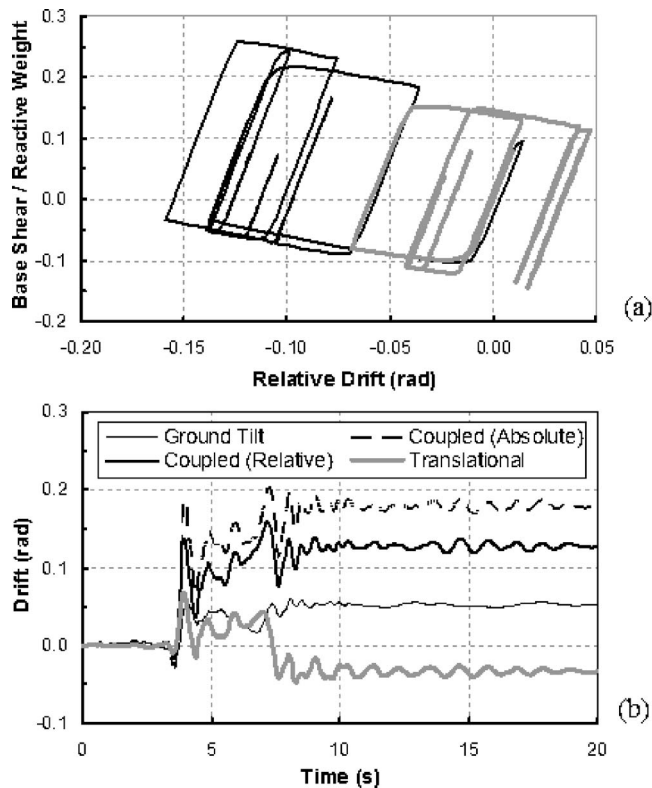


Fig. 11. Comparison of ground tilt and structural drift (unlike relative drift, absolute drift includes rigid body rotation)

inclusion of tilt motion during the response analysis results in noticeable asymmetric deformation in the direction of ground tilting. One of the consequences of asymmetric deformation is the large displacement demand and resultant higher ductility demand. The maximum ductility created by the coupled motion reach 12.3, whereas it remains only 4.7 when the tilt effects are not accounted for. Another important aspect of including tilt in the analysis is the obtained larger residual drift. Fig. 11(b) compares the drift time histories for the SDOF oscillator excited by coupled and translational motions in a separate fashion. There is an evident difference in residual relative drift created due to coupled motion and drift initiated by translational motion alone. When the absolute drift (relative drift+ground tilt) is computed, this difference becomes even more dramatic. As the ground motion ceases, the SDOF oscillator excited by translational component remained in the tilted position with only 1.9° , while considering ground tilting results in 7.3° relative and 10.3° absolute inclination of the oscillator. If the maximum deformation demand is considered as a performance evaluation criterion, one neglects the big difference in the behavior that a system exhibits with and without considering tilt during a seismic excitation. Thus a systematic approach is needed for a new design or for evaluation of existing structures when dealing with tilt in the ground surface.

Spectral Period Independent $P-\Delta$ Parameter

The regular response spectra of ground motion present seismic demands per unit mass. Therefore, for representation of the $P-\Delta$ effects in a spectral format, an equivalent structure loaded by only dead load (i.e., reactive weight, W) is derived through Eq. (8), and live load components are intentionally not included in the formu-

lation. The $P-\Delta$ effects are often characterized by the constant stability coefficient, θ in the response spectrum (e.g., Bernal 1987; MacRae 1994). However, θ varies with change in system stiffness as implied by Eq. (7). In other words, θ is a function of spectral period; therefore it cannot serve as a convenient parameter to be used directly in a spectral format unless l (height or length of oscillator) is varied at each spectral period to keep θ constant. Therefore, there is a need for a new descriptor that can be invariantly used in generating response spectrum and also adequately represents $P-\Delta$ effects.

Let us consider again a SDOF system under the influence of $P-\Delta$ force-couple only [or $P-\Delta$ moment as illustrated in Fig. 7(b)]. Note that such a system has exactly the same behavior of a simple pendulum where the driven force to initiate motion is created by the reactive weight only. This driven force can be expressed as

$$F_{P-\Delta} = mg \frac{u}{l} = k_G u \quad (13)$$

in which it is possible to directly extract *geometric oscillation period* of the oscillator as

$$T_G = 2\pi \sqrt{\frac{l}{g}} \quad (14)$$

T_G in Eq. (14) is the same as the oscillation period of a simple pendulum with length of l , although gravitational force acts in stabilizing the motion for pendulum unlike its destabilizing effects for a SDOF oscillator (or inverted pendulum). The squared ratio of elastic vibration period T_0 to *geometric oscillation period* (T_G) defines the stability coefficient alternatively as

$$\theta = k_G/k_0 = (T_0/T_G)^2 \quad (15)$$

If the right-hand side of the Eq. (15) is plugged into Eq. (8), one can easily derive the relation between effective period of the system and *geometric oscillation period* as in the following:

$$T = T_0 T_G / \sqrt{T_G^2 - T_0^2} \quad (16)$$

Importantly, Eq. (16) indicates that if the *geometric oscillation period* of the system (T_G) is equal or smaller than the initial elastic period (T_0), the instability (i.e., $\theta \geq 1.0$) in the system is initiated. For stable system, *geometric oscillation period* should be always greater than the initial elastic period. Therefore, T_G can serve as an effective tool to prevent geometric instability by quantifying the lower-bound limit for lateral stiffness, which essentially defines the elastic vibration period of a SDOF oscillator. It should be emphasized that T_G is an invariant quantity for a SDOF oscillator with a given l (height), and it is independent of initial stiffness, thus the system initial period (T_0). That turns *geometric oscillation period* (T_G) as a convenient representative $P-\Delta$ parameter to be used directly in a spectral format in lieu of well-know stability coefficient θ .

Coupled Tilt and Translational Ground Motion Response Spectra

Following the conceptual development of an invariant stability parameter to be used in a spectral format, both elastic and inelastic systems with constant ductility demands are examined to identify those situations in which the overall response is likely to receive significant contributions from the tilt component of ground motion. For this purpose, parallel to regular response

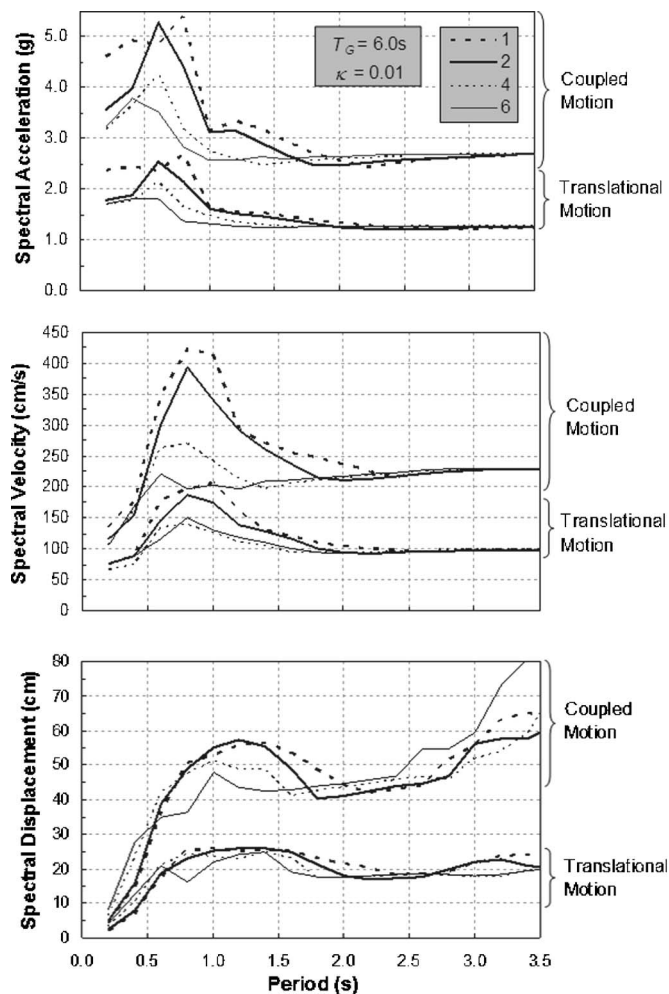


Fig. 12. Comparison of constant-ductility response spectra

spectra, CTT ground motion response spectra are generated at constant ductility levels ($\mu=1, 2, 4$, and 6) as a function of T , damping coefficient (5%) and T_G . When the seismic performance of the structure is assessed by using the maximum ductility demand as an evaluation criterion, constant ductility spectra will augment understanding the effects of tilt component on the inelastic structural performance.

As portrayed in Fig. 12, spectral response quantities of interest are the relative displacement of a SDOF system and its time derivatives. The constant-ductility spectra are generated for the Pacoima Dam record considering stable bilinear hysteretic model with κ (postyield stiffness ratio) equal to 0.01 and viscous damping equal to 5 percent of critical damping. The plot corresponding to elastic response has $\mu=1$. The $P-\Delta$ effects for all cases are represented by a constant value of the *geometric oscillation period* of (T_G) 6.0 s. The selected value of T_G is directly related to a physical system (corresponding to a typical highway bridge bent example given by Chopra and Goel 2001).

The tilt component, when it is coupled with translational motion, amplifies all response quantities regardless of spectral period. The difference between two cases becomes more pronounced as the spectral period increases. At the period of 3.5 s, coupling of tilt and translational motion yields more than 3 times larger spectral displacement demand compared to displacement demand imposed by pure translational motion. As Eq. (11) implies, tilt effects are inherently conditioned on the height of the

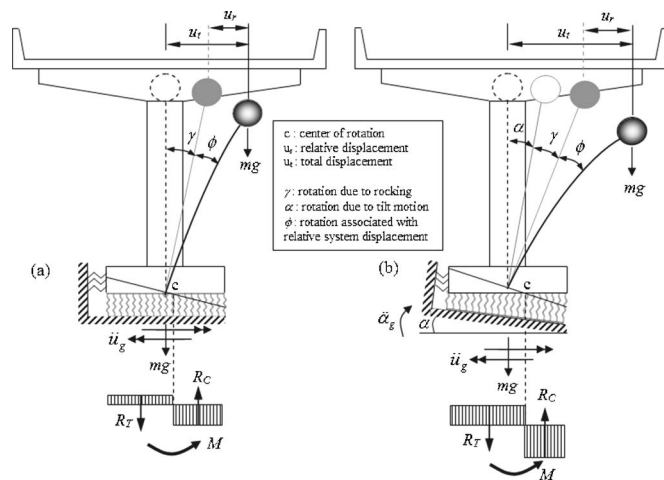


Fig. 13. Idealized behavior of single bridge bent under (a) pure translation motion; (b) coupled tilt and translational motion considering SSI [assuming that compression (R_C) and tension forces (R_T) at soil-footing interface have a rigid plastic interface pressure distribution]

system, and the difference observed in Fig. 12 indicates that ground tilting larger than few degrees can be most detrimental, particularly for long and flexible structures.

As shown in Fig. 3(a), the dominant period of the translational motion is 1 s, which also coincides with the predominant period of tilt motion at which the peak Fourier amplitude is computed (see Fig. 6). Not surprisingly, the peak response takes place around this period in the velocity spectrum. By comparing spectra in Figs. 12(a–c), it can be also concluded that the effect of tilt motion tends to be more important in SDOF systems developing larger values of μ_{\max} . Nevertheless, in some cases, particularly for a SDOF system with T close to predominant period of motion and developing a smaller μ_{\max} , the effect of tilt is still noticeable.

Coupling of Tilting Excitation with Rocking Response

SDOF response to coupled tilt and translational motions and generation of CTT spectrum were derived [see Eq. (12)] considering a superstructure response only. Specifically, the tilt and translational motions are assumed to be direct inputs. However, the approach can be advanced to cover the coupling of tilting excitation with the respective rocking response induced by SSI. In fact, response of slender structures is usually governed by the large overturning moment at their base due to longer lever arm they have. If rocking and uplift may occur (associated with the translational motion), this moment is then reduced by the stabilizing moment produced by the subgrade reaction against the destabilizing moment created by gravity. In many earthquakes, a number of structures had responded to a seismic excitation by rocking on their foundation, and in some cases, this enabled them to avoid failure. Therefore, SSI creates an insulation effect against the strong shaking of earthquake. The rocking response is particularly of interest for bridge piers, which often present geometry, mass distribution and foundation characteristics that could favor a controlled rocking response. Fig. 13(a) illustrates the rocking behavior of a simple bridge bent excited by the horizontal motion. Also shown is the stabilizing moment created at the foundation level.

The coupling of ground tilting with rocking response makes the problem even more complicate. As evident from Eq. (11) that dynamic ground tilting may create large overturning moment by amplifying the base shear. The amplitude of amplification depends on the effective height and also the intensity of angular acceleration. If the foundation is not flexible enough to accommodate this additional moment by allowing adequate rocking response, base shear may reach to a critical value. For bridge pier, for instance, plastic hinge may initiate between foundation and pier base to dissipate the input energy due to the large overturning moment. Therefore, when tilting and horizontal motions are coupled with the rocking response [see Fig. 13(b)], they may result in enhanced permanent tilting of a structure compared to a structure excited by pure horizontal motion [Fig. 13(a)]. The severity of such an interaction depends on the phasing of rocking response with the tilting excitation. If they act out-of-phase with respect to each other, then the rocking response may help to reduce the effects of angular acceleration. On the other hand, reverse may happen in case of in-phase response of rocking with angular acceleration which may eventually create large dynamic and permanent tilting.

The level of remediation (i.e., amount of stabilizing moment) due to rocking is not only directly related to the dimensions of a spread footing but also subgrade stiffness as well as superstructure response characteristics. Its strong dependency on soil and structure specific parameters turns its generic representation within a spectral format (or in CTT spectrum) impractical. However, coupling of rocking motion with tilting excitation can be explicitly considered in design through utilizing CTT spectrum (including $P-\Delta$ effects) and accounting for (1) period elongation and (2) change in system damping associated with foundation flexibility. FEMA-440 (ATC 2005) now provides detailed information on the explicit implementation of SSI effects in performance-based design where the hazard spectrum computed using fixed-base oscillator is modified due to change in damping ratio. In this procedure, the period shifting due to rocking response is also considered. Without departing from the same design principles, the CTT spectrum can be used in lieu of a hazard spectrum. Thereby, the important $P-\Delta$ effects and coupling of tilting excitation with translational motion will be implemented in design or performance assessment without disregarding the remedial effects of SSI.

Summary and Conclusions

In the conventional approach, structures are designed to resist only horizontal translational motions as the representation of strong earthquake impact. Occasionally in the design, the vertical component of excitation is considered for structures with long spans such as bridges; however, rotational components of ground excitation are almost always ignored. Many structural failures and the damage caused by earthquakes can be linked to differential and rotational ground motions. Torsional responses of tall buildings in Los Angeles during the San Fernando, California Earthquake in 1971 could be attributed to torsional excitation (Hart et al. 1975), while rotational and longitudinal differential motions may have caused the collapse of bridges during San Fernando 1971, Miyagi-ken-Oki 1978 (Bycroft 1980) and Northridge 1994 (Trifunac et al. 1996) earthquakes. Earthquake damage to pipelines that is not associated with faulting or landslides, but is due to large differential motions and strains in the soil, reflects the consequences of propagating seismic waves and of the associated

large rotations and twisting of soil blocks caused by lateral spreads and early stages of liquefaction (Ariman and Muleski 1981; Trifunac and Todorovska 1998). Despite these evidences, there are practically no measurements of rotations during earthquake strong ground motion, and existing data are limited to indirect estimates based on special techniques (extracting rotation information from seismic sensors or closely spaced arrays not specifically designed for rotation measurements).

In this study, a simple yet effective technique is presented to explicitly recover the rotational motions from recorded horizontal accelerograms. The procedure can only be applied to the uncorrected (unprocessed) records (usually called Vol. 0 or Vol. 1). The only change allowed is the correction for the sensitivity. Some digital recorders automatically perform filtering of data (preprocessing) that most likely results in losing long-period information related to tilts, therefore absolutely no filtering should be applied to the recorded data prior to applying the proposed procedure. The methodology is verified through comparisons with field measurement at the Pacoima Dam—Upper Abutment station, and a reasonable estimate of residual tilt is obtained.

Compared to 3.1° tilt at the Pacoima Dam—upper left abutment, the record at the Pacoima Dam—downstream (CSMIP St. No. 24207) resulted in a tilt of about 0.80° along one of the horizontal components. Another record, Pacoima Dam—Kagel Canyon, did not result in tilt. Based on comparison with records taken from other stations near the upper left abutment station, it is possible to conclude that relatively large tilts of up to a few degrees are most likely associated with local geological and topographical site effects. Thus, one can conclude that tilt of about 3.1° was actually a local site effect induced by strong shaking.

The dynamic response of earthquake-resistant structures cannot be understood unless a systematic consideration of the tilt component of seismic excitation is made. Coupling of translational motion with tilt motion, frequency content of these components and their interaction with dynamic characteristics of the structure and soil are primary factors affecting the response. Many of these factors are investigated in the course of this paper using elastic and inelastic SDOF oscillators. In some cases maximum ductility of SDOF oscillators subjected to coupled tilt and translational motion doubled the ductility demand imposed by pure translational motion. This significant difference indicates that the tilt component of ground motion may strongly affect the damage suffered by earthquake-resistant structures originally designed for certain ductility demands accounting for translational records only.

Parallel to amplified displacement demand, structures exhibiting tilt may have a tendency to show asymmetric yielding. It means, due to residual base tilting, the structure may continue to be excited by the ground motion in a tilted position. In such case, any inertial forces larger than a certain threshold may easily create additional asymmetrically accumulated inelastic deformation. It is also shown in this paper that $P-\Delta$ effects associated with tilt motion can cause the system to deform beyond a yield point and create negative tangent stiffness in the postyield deformation range. If these secondary geometric effects reach certain limits (i.e., θ approaches 1.0), they may trigger dynamic instability by leading to large pseudo-static shears and moments. For these reasons, the rotational component of ground motion can be critical, particularly for long and flexible moment frame buildings, towers and elevated water tanks where the height of the structure determines the severity of secondary moments and inertia forces caused by angular acceleration.

To address the overall impacts of rotational components in a

systematic manner, this paper advances the concept of a coupled tilt and translational (CTT) ground motion response spectrum. The CTT spectrum plots values of peak response parameters versus time or frequency, and it is a distinct and valuable intensity measure of earthquakes by providing information on the shaking that is not identifiable by the response spectrum alone. The intensity of tilt effects in the CTT spectrum is represented by a new index, called the *geometric oscillation period*. This representation is useful as it can be estimated accurately based on the information available early in the design. The CTT spectrum, created using an equivalent fixed-base SDOF oscillator, has the potential to be used in design in a manner analogous to use of a response spectrum since strengths can be established directly considering tilt effects in a single step.

Acknowledgments

The writers would like to thank three anonymous reviewers for their suggestions which improved the technical quality of the paper. Any opinions, findings, and conclusions or recommendations expressed in this material are those of the writers and do not necessarily reflect the views of the California Geological Survey.

References

- Applied Technology Council. (2005). "Improvement of nonlinear static seismic analysis procedures (FEMA 440)" *Prepared for FEMA under ATC-55 Project*, Redwood City, Calif.
- Ariman, T., and Muleski, G. E. (1981). "A review of the response of buried pipelines under seismic excitation." *Earthquake Eng. Struct. Dyn.*, 9(2), 133–152.
- Bernal, D. (1987). "Instability of buildings subjected to earthquakes." *Eng. Struct.*, 20(4–6), 496–502.
- Bouchon, M., and Aki, K. (1982). "Strain, tilt, and rotation associated with strong ground motion in the vicinity of earthquake faults." *Bull. Seismol. Soc. Am.*, 72, 1717–1738.
- Bycroft, G. N. (1980). "Soil-foundation interaction and differential ground motions." *Earthquake Eng. Struct. Dyn.*, 8(5), 397–404.
- Castellani, A., and Boffi, G. (1986). "Rotational components of the surface ground motion during an earthquake." *Earthquake Eng. Struct. Dyn.*, 14(5), 751–767.
- Chopra, A. K., and Goel, R. K. (2001). "Direct displacement-based design: Use of inelastic vs. elastic design spectra." *Earthquake Spectra*, 17(1), 47–64.
- Ghafari-Ashtiani, M., and Singh, M. P. (1986). "Structural response for six-correlated earthquake components." *Earthquake Eng. Struct. Dyn.*, 14(1), 103–119.
- Graizer, V. M. (1989). "Bearing on the problem of inertial seismometry." *Izv. Acad. Sci., USSR, Phys. Solid Earth*, 25(1), 26–29.
- Graizer, V. M. (2005). "Effect of tilt on ground motion data processing." *Soil Dyn. Earthquake Eng.*, 25(3), 197–204.
- Graizer, V. M. (2006a). "Equation of pendulum motion including rotations and its implications to the strong-ground motion." *Earthquake source asymmetry, structural media, and rotation effects*, Monograph, 471–491.
- Graizer, V. M. (2006b). "Tilts in strong ground motion." *Bull. Seismol. Soc. Am.*, 96(6), 2090–2102.
- Gupta, V. K., and Trifunac, M. D. (1991). "Seismic response of multistoried buildings including the effects of soil-structure interaction." *Soil Dyn. Earthquake Eng.*, 10(8), 414–422.
- Hao, H., Olivera, C. S., and Pazien, J. (1989). "Multiple-station ground motion processing and simulations based on SMART-1." *Nucl. Eng. Des.*, 111(3), 293–310.
- Harichandran, R. S. (1991). "Estimating the spatial variation of earthquake ground motion from dense array recordings." *Struct. Safety*, 10(1–3), 219–233.
- Hart, G. C., Lew, M., and DiJulio, M. (1975). "Torsional response of high-rise buildings." *J. Struct. Div.*, 101(2), 397–416.
- Kalkan, E., and Kunnath, S. K. (2006). "Effects of fling-step and forward directivity on the seismic response of buildings." *Earthquake Spectra*, 22(2), 367–390.
- Kalkan, E., and Kunnath, S. K. (2007). "Effective cyclic energy as a measure of seismic demand." *J. Earthquake Eng.*, 11(5).
- Lee, V. W. (1979). "Investigation of three-dimensional soil-structure interaction." *Rep. No. CE79-11*, Univ. of Southern California, Los Angeles.
- Lee, V. W., and Trifunac, M. D. (1985). "Torsional accelerograms." *Soil Dyn. Earthquake Eng.*, 4(3), 132–142.
- Lee, V. W., and Trifunac, M. D. (1987). "Rocking strong earthquake accelerations." *Soil Dyn. Earthquake Eng.*, 6(2), 75–89.
- Li, H., Sunb, L. Y., and Wanga, S. Y. (2004). "Improved approach for obtaining rotational components of seismic motion." *Nucl. Eng. Des.*, 232(2), 131–137.
- MacRae, G. A. (1994). "P-D effects on single-degree-of-freedom structures in earthquakes." *Earthquake Spectra*, 10(3), 539–568.
- Niazi, M. (1986). "Inferred displacements, velocities and rotations of a long rigid foundation located at El Centro differential array site during the 1979 Imperial Valley, California earthquake." *Earthquake Eng. Struct. Dyn.*, 14(4), 531–542.
- Nigbor, R. L. (1994). "Six-degree of freedom ground motion measurement." *Bull. Seismol. Soc. Am.*, 84(4), 1665–1669.
- Oliveira, C. S., and Bolt, B. A. (1989). "Rotational components of surface strong ground motion." *Earthquake Eng. Struct. Dyn.*, 18(4), 517–526.
- Shakal, A., Cao, T., and Darragh, R. (1994). "Processing of the upper left abutment record from Pacoima dam for the Northridge Earthquake." *Rep. No. OSMS 94-13*, Sacramento, Calif.
- Stratta, J. L., and Griswold, T. F. (1976). "Rotation of footing due to surface waves." *Bull. Seismol. Soc. Am.*, 66(1), 105–108.
- Takeo, M., and Ito, H. M. (1997). "What can be learned from rotational motions excited by earthquakes?" *Geophys. J. Int.*, 129, 319–329.
- Todorovska, M. I. (1998). "Cross-axis sensitivity of accelerographs with pendulum like transducers—Mathematical model and the inverse problem." *Earthquake Eng. Struct. Dyn.*, 27(10), 1031–1051.
- Trifunac, M. D. (1971). "Zero baseline correction of strong motion accelerograms." *Bull. Seismol. Soc. Am.*, 61(5), 1201–1211.
- Trifunac, M. D., and Hudson, D. E. (1971). "Analysis of the Pacoima dam accelerogram—San Fernando, California, earthquake of 1971." *Bull. Seismol. Soc. Am.*, 61(5), 1393–1411.
- Trifunac, M. D., and Todorovska, M. I. (1998). "Non-linear soil response as a natural passive isolation mechanism—The 1994 Northridge, California Earthquake." *Soil Dyn. Earthquake Eng.*, 17(1), 41–51.
- Trifunac, M. D., and Todorovska, M. I. (2001). "A note on the usable dynamic range of accelerographs recording translation." *Soil Dyn. Earthquake Eng.*, 21(4), 275–286.
- Trifunac, M. D., Todorovska, M. I., and Ivanovic, S. S. (1996). "Peak velocities, and peak surface strains during Northridge, California earthquake of 17 January 1994." *Soil Dyn. Earthquake Eng.*, 15(5), 301–310.
- Tselentis, G.-A., and Makropoulos, K. C. (1986). "Rates of crustal deformation in the Gulf of Corinth [central Greece] as determined from seismicity." *Tectonophysics*, 124(1–2), 55–66.
- Wong, H. L., and Trifunac, M. D. (1977). "Effect of cross-axis sensitivity and misalignment on response of mechanical-optical accelerographs." *Bull. Seismol. Soc. Am.*, 67(3), 929–956.
- Zahradnik, J., and Plesinger, A. (2005). "Long-period pulses in broadband records of near earthquakes." *Bull. Seismol. Soc. Am.*, 95(5), 1928–1939.
- Zerva, A., and Beck, J. L. (2003). "Identification of parametric ground motion random fields from spatially recorded seismic data." *Earthquake Eng. Struct. Dyn.*, 32(5), 771–791.